

This article was downloaded by:

On: 23 January 2011

Access details: *Access Details: Free Access*

Publisher *Taylor & Francis*

Informa Ltd Registered in England and Wales Registered Number: 1072954 Registered office: Mortimer House, 37-41 Mortimer Street, London W1T 3JH, UK



## Journal of Coordination Chemistry

Publication details, including instructions for authors and subscription information:

<http://www.informaworld.com/smpp/title~content=t713455674>

### Investigations of Polyoxometalates in Aqueous Solutions. I. The Formation of $Al_{13}(OH)_{31}^{7+}$ Cation

Francesco Salvatore<sup>a</sup>; Marco Trifuoggi<sup>a</sup>

<sup>a</sup> Dipartimento di Chimica, Università di Napoli "Federico II", Napoli, Italy

**To cite this Article** Salvatore, Francesco and Trifuoggi, Marco(2006) 'Investigations of Polyoxometalates in Aqueous Solutions. I. The Formation of  $Al_{13}(OH)_{31}^{7+}$  Cation', *Journal of Coordination Chemistry*, 51: 2, 271 – 282

**To link to this Article:** DOI: 10.1080/00958970008055133

**URL:** <http://dx.doi.org/10.1080/00958970008055133>

PLEASE SCROLL DOWN FOR ARTICLE

Full terms and conditions of use: <http://www.informaworld.com/terms-and-conditions-of-access.pdf>

This article may be used for research, teaching and private study purposes. Any substantial or systematic reproduction, re-distribution, re-selling, loan or sub-licensing, systematic supply or distribution in any form to anyone is expressly forbidden.

The publisher does not give any warranty express or implied or make any representation that the contents will be complete or accurate or up to date. The accuracy of any instructions, formulae and drug doses should be independently verified with primary sources. The publisher shall not be liable for any loss, actions, claims, proceedings, demand or costs or damages whatsoever or howsoever caused arising directly or indirectly in connection with or arising out of the use of this material.

## INVESTIGATIONS OF POLYOXOMETALATES IN AQUEOUS SOLUTIONS. I. THE FORMATION OF $\text{Al}_{13}(\text{OH})_{32}^{7+}$ CATION

FRANCESCO SALVATORE\* and MARCO TRIFUOGGI

*Dipartimento di Chimica, Università di Napoli "Federico II",  
via Mezzocannone 4, 80134 Napoli, Italy*

*(Received 27 October 1999)*

The formation of polyhydroxo aluminum(III) complexes has been investigated at 30°C and in a 3 M (K)Cl ionic medium by p[H] measurements. The uncommon "integral titration" technique employed has enabled measurements of oversaturated solutions up to  $\text{OH}^-$  to Al(III) ratios as large as 2.65. This has allowed the detection of the undescribed species  $\text{Al}_{13}(\text{OH})_{35}^{4+}$ . The data can very satisfactorily be explained by assuming the species  $\text{Al}_2(\text{OH})_2^+$ ,  $\text{Al}_3(\text{OH})_6^{3+}$ ,  $\text{Al}_{13}(\text{OH})_{32}^{7+}$ , and  $\text{Al}_{13}(\text{OH})_{35}^{4+}$ . The Al(III) concentration has been changed from  $\approx 0.0025$  to  $\approx 0.040$  M and the spacings of the titration curves at different aluminum levels are a clear and direct evidence for the formation of  $\text{Al}_{13}(\text{OH})_{32}^{7+}$ , which dominates the hydrolysis products. The data presented in this paper are best accounted for if the trimer  $\text{Al}_3(\text{OH})_6^{3+}$  is substituted for  $\text{Al}_3(\text{OH})_4^{5+}$  which is frequently reported. The formation of the "13" cations may result from the reaction of four  $\text{Al}_3(\text{OH})_6^{3+}$  with a transient  $\text{Al}(\text{OH})_4^-$  species which is formed, upon addition of a rather concentrated basic solution, owing to a local excess of  $\text{OH}^-$ .

**Keywords:** Hydrolysis; aluminum; polyoxometalates; metal clusters

### INTRODUCTION

The hydrolysis of  $\text{Al}^{3+}$  cation has been of interest for at least a century, and fundamental work, up to 1975, is reviewed by Baes and Mesmer.<sup>1</sup> Discussion of aluminum(III) hydrolysis has nevertheless not ceased and is a topic in a vast number of investigations of  $\text{Al}^{3+}$  complexes,<sup>2–4</sup> undertaken to elucidate the role of aluminum in natural and biological systems. Polymeric hydroxo complexes which dominate the complex hydrolysis mechanism of

\* Corresponding author.

aluminum(III) are also extensively used in many areas of material science as building blocks for the synthesis of new materials.<sup>5,6</sup> Present understanding of aluminum(III) hydrolysis indicates that mononuclear hydroxo complexes, presumably produced during the early stages of hydrolysis, readily condense, *via* repeated olation, to polynuclear complexes in which hydroxo bridges ("ol" bridges) are formed between metal centres.

A discouragingly large number of species have however been reported.<sup>1,7</sup> In addition to  $\text{Al}(\text{OH})^{2+}$ ,  $\text{Al}(\text{OH})_2^+$ ,  $\text{Al}(\text{OH})_3$ , and  $\text{Al}(\text{OH})_4^-$  (which clearly dominate at very low Al(III) concentrations in solutions saturated with  $\text{Al}(\text{OH})_3(\text{s})$ ), evidence for  $\text{Al}_2(\text{OH})_2^{4+}$ ,  $\text{Al}_2(\text{OH})_4^{2+}$ ,  $\text{Al}_3(\text{OH})_4^{5+}$ ,  $\text{Al}_4(\text{OH})_8^{4+}$ ,  $\text{Al}_7(\text{OH})_{16}^{5+}$ ,  $\text{Al}_7(\text{OH})_{17}^{4+}$ ,  $\text{Al}_{13}(\text{OH})_{34}^{5+}$ ,  $\text{Al}_{14}(\text{OH})_{34}^{8+}$ , *etc.*, has been produced from time to time under a variety of ionic media, temperatures and aluminum concentrations. The slowness of polyhydroxo complex formation reactions has often been invoked to explain discrepancies in the data from different laboratories and has inspired investigations under rather unusual experimental conditions (temperature up to  $149^\circ\text{C}$ <sup>8</sup> and equilibration times of several months<sup>2</sup> have been employed).

By taking a purely statistical point of view,  $\text{Al}_2(\text{OH})_2^{4+}$  and  $\text{Al}_3(\text{OH})_4^{3+}$  are the most frequently reported small polynuclear complexes, while the cation  $\text{Al}_{13}(\text{OH})_{32}^{7+}$  (the "13, 32" cation) is most often postulated as the final product of the polymerization process. From hydrolysed solutions of  $\text{AlCl}_3$  at high temperatures a sulphate can be precipitated which has been found to contain  $\text{Al}_{13}(\text{OH})_{32}^{7+}$  units, whose very bulky structure has been determined by X-ray crystallography.<sup>9</sup> A qualitative model for the formation of  $\text{Al}_{13}(\text{OH})_{32}^{7+}$ , from the precursor  $[\text{Al}_3(\text{tris-}\mu\text{-OH})(\text{OH})_3]^{5+}$ , where *tris-}\mu\text{-OH}* emphasizes that one OH ligand bridges three aluminums, has been presented by Wood.<sup>5</sup> Although this model is inspiring, neither the existence of  $\text{Al}_{13}(\text{OH})_{32}^{7+}$ , nor its precursors has admittedly<sup>1</sup> been clearly demonstrated from direct measurements of aqueous solutions at room temperatures.

At present the hydrolysis mechanism of aluminum(III) is neither black nor white, but, depending on one's point of view, to a variable extent, grey. The reason for this state of affairs are the many inadequacies of equilibrium analysis methodology to manage successfully the problem of the formation of polynuclear hydroxo species in solution.

Olation is the unavoidable consequence of hydrolysis and would generally occur when metal cation solutions are hydrolysed to such an extent to produce sufficient concentrations of monomeric hydroxo species, which are the building blocks of polynuclear hydroxo complexes. However, the polymerization process is generally interrupted by the precipitation of metal hydroxides which leaves such low concentrations of monomers in solution

that polymeric species cannot be observed at equilibrium. An obvious corollary of this is that polymeric hydroxo complexes occur generally in oversaturated solutions as transient species of variable lifetime. This does not decrease our interest in their formation because they can and are employed as reactants in synthetic schemes which operate on a time scale shorter than the precipitation. Fundamentally, present methodology of hydrolysis investigations (mainly p[H] titrations) cannot cope with this problem because the time scale of the equilibrium analysis experiment is much longer than the lifetime of the sought species. In this paper we present equilibrium analysis experiments, to which we will apply the term "integral titrations", with a time scale of a few minutes, which compares favourably with the several hours time scale of usual incremental titrations.

The results of this investigation rest on two basic assumptions:

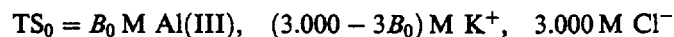
- (1) the precipitation of aluminum hydroxide is slow enough at room temperature so that a lag-time period exists between mixing an acidic  $\text{Al}^{3+}$  solution with the titrating base and the formation of detectable amounts of solid (that is to say that the lifetime of the species formed by the reaction of  $\text{Al}^{3+}$  with  $\text{OH}^-$  is at least a few minutes);
- (2) the reaction between  $\text{Al}^{3+}$  and  $\text{OH}^-$  reaches equilibrium before the lag-time period is elapsed (*i.e.*, homogeneous equilibrium is established although solutions may not be in equilibrium with respect to the precipitation of aluminum hydroxide or of some other solid phase).

Although we strictly cannot invoke any direct justification for this, the results presented in the following paper show that these assumptions must be substantially correct.

## EXPERIMENTAL

### Methods

The hydrolysis of  $\text{Al}^{3+}$  ion has been investigated at  $30^\circ\text{C}$  and in a 3 M (K)Cl ionic medium, in the range of aluminum concentrations,  $B$ , between 0.00253 and 0.04024 M by p[H] measurements with a combined pH glass electrode. An acidic solution of  $\text{AlCl}_3$ ,  $\text{TS}_0$ , having the following general initial analytical composition



was titrated with KOH titrant solution, T, of composition

$$T = 0.1000 \text{ M KOH, } 3.000 \text{ M KCl.}$$

Five titrations have been performed in which  $B_0$  had the values 0.00253, 0.00525, 0.00977, 0.02070 and 0.04024 M. The general composition of the measured solution, TS, was

$$TS = BM \text{ Al(III), } A \text{ M OH}^-, (3.000 + A - 3B) \text{ M K}^+, 3.000 \text{ M Cl}^-$$

An "integral titration" technique has been employed. An integral titration consists in adding for each point of the titration curve the whole titrant volume,  $V_T$ , to the initial volume,  $V_0$ , of titrated solution. In practice, after measurement of the point of the titration curve corresponding to  $V_T$ , the titration is restarted with a fresh volume  $V_0$  of titrated solution, to which the whole volume ( $V_T + \Delta V_T$ ) of titrant, corresponding to the next point of the titration curve, is added (not only the increment  $\Delta V_T$  as in usual incremental titrations).

The advantage of integral titrations is that their time scale is very short, being that of a single p[H] measurement, although the time necessary to obtain the titration curve is actually very long. This is because the measurement of each point of the titration curve restarts at zero time. The same principle underlies polarographic techniques where the time scale is governed by the drop time of the dropping mercury electrode rather than by the time actually required to record a polarogram. Nevertheless the appearance and the meaning of the integral titration curve are exactly the same as that of an incremental titration curve. During the titration of the solution of a metal cation with a base, in order to obtain the integral titration curve, it is only necessary that the time-lag separating the mixing of solutions and the formation of a precipitate be of the order of the equilibration time of the glass electrode. This is obviously a much less restrictive requirement compared to that of an incremental titration, which would require the titrated solution be kept in an oversaturated state for a few hours.

The five integral titration curves measured during this investigation are presented in Figure 1, as p[H] vs  $f$ , where  $f = A/B$ , is the titrated fraction of metal cation. The experimental data in the form ( $-\log B$ ,  $-\log A$ , p[H]) are reported in Table I and will be the basis of following calculations.

### p[H] Measurements

Integral titrations were performed by using a fully automated apparatus based on Metrohm piston dosing burettes and a combined glass electrode

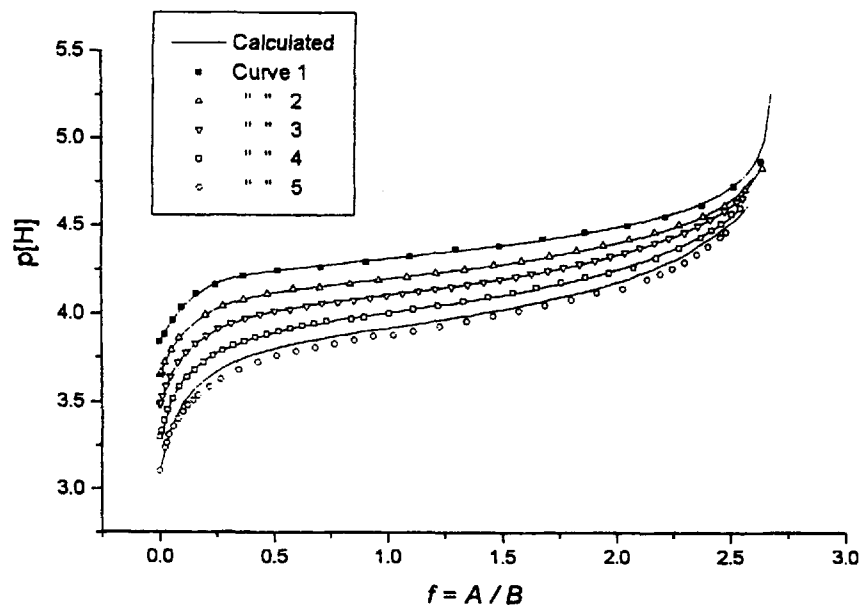


FIGURE 1 Graphical presentation of the results. Points represent  $p[H]$  vs  $f$  experimental data of Table I ( $f = A/B$ ); full curves have been calculated with the species and the constants given in Table II. Numbers on curves identify different initial concentration,  $B_0$ , of  $Al(III)$ , as reported in Table II.

under Metrohm 706 microprocessor control. The predefined volumes of  $TS_0$  and  $T$ , previously thermostatted at  $30 \pm 1^\circ C$ , were delivered to a thermostatted ( $30.00 \pm 0.05^\circ C$ ) titration vessel by triggering the microprocessor and rapidly mixed with a magnetic stirrer. After mixing, the microprocessor immediately started the measurements at short time intervals. The measurements were sent to a printer which recorded  $p[H]$  vs time. In a few minutes the time curve reached a *plateau* with a negligible slope over an observation period of about 10 min, at which time measurements were discontinued. Only in the case of the titration at  $B_0 = 0.04024 M$  (curve 5 in Figure 1) a measurable drift of the  $p[H]$  towards acidic values was observed after mixing. We interpret this as resulting from precipitation of a solid phase, but performed in any case the titration by taking the  $p[H]$  readings after 10 min from mixing.

The precision of the measured  $p[H]$  and of the delivered volumes was respectively 0.001  $p[H]$  units and  $0.001 cm^3$ .

The combined glass electrode was Metrohm model 6.0232.100 which has a very short response time and a 3 M KCl double liquid junction. In practice

TABLE I Summary of the experimental data. The five titrations are identified from the initial concentration of aluminum,  $B_0$ , in the titrated solution

---

$B_0 = 0.00253$  M: ( $-\log B$ ,  $-\log A$ ,  $p[H]$ ) curve 1 of Figure 1;  
 2.596<sub>8</sub>,  $A = 0$ , 3.843; 2.597<sub>1</sub>, -4.267<sub>8</sub>, 3.885; 2.597<sub>5</sub>, 3.848<sub>3</sub>, 3.965; 2.597<sub>9</sub>, 3.620<sub>8</sub>, 4.028;  
 2.598<sub>7</sub>, 3.382<sub>7</sub>, 4.106; 2.600<sub>0</sub>, 3.196<sub>5</sub>, 4.165; 2.600<sub>9</sub>, 3.030<sub>9</sub>, 4.209; 2.602<sub>6</sub>, 2.883<sub>8</sub>, 4.237;  
 2.604<sub>6</sub>, 2.753<sub>4</sub>, 4.264; 2.606<sub>7</sub>, 2.649<sub>6</sub>, 4.292; 2.608<sub>8</sub>, 2.567<sub>0</sub>, 4.322; 2.610<sub>9</sub>, 2.498<sub>3</sub>, 4.351;  
 2.612<sub>9</sub>, 2.440<sub>0</sub>, 4.384; 2.614<sub>9</sub>, 2.390<sub>0</sub>, 4.419; 2.616<sub>9</sub>, 2.346<sub>3</sub>, 4.458; 2.618<sub>8</sub>, 2.308<sub>1</sub>, 4.503;  
 2.620<sub>6</sub>, 2.275<sub>2</sub>, 4.554; 2.602<sub>2</sub>, 2.246<sub>2</sub>, 4.615; 2.623<sub>7</sub>, 2.222<sub>0</sub>, 4.730; 2.625<sub>0</sub>, 2.202<sub>6</sub>, 4.865

$B_0 = 0.005248$  M: ( $-\log B$ ,  $-\log A$ ,  $p[H]$ ) curve 2 of Figure 1;  
 2.280<sub>0</sub>,  $A = 0$ , 3.648; 2.280<sub>1</sub>, -4.602<sub>2</sub>, 3.655; 2.280<sub>2</sub>, 4.426<sub>1</sub>, 3.663; 2.280<sub>5</sub>, 3.912<sub>3</sub>, 3.716;  
 2.281<sub>1</sub>, 3.573<sub>8</sub>, 3.794; 2.281<sub>9</sub>, 3.351<sub>1</sub>, 3.859; 2.284<sub>6</sub>, 2.977<sub>2</sub>, 3.990; 2.286<sub>3</sub>, 2.839<sub>0</sub>, 4.039;  
 2.288<sub>4</sub>, 2.718<sub>4</sub>, 4.077; 2.290<sub>7</sub>, 2.613<sub>6</sub>, 4.108; 2.293<sub>2</sub>, 2.523<sub>5</sub>, 4.135; 2.295<sub>8</sub>, 2.447<sub>0</sub>, 4.145;  
 2.298<sub>8</sub>, 2.374<sub>5</sub>, 4.166; 2.301<sub>5</sub>, 2.316<sub>4</sub>, 4.187; 2.304<sub>2</sub>, 2.266<sub>6</sub>, 4.207; 2.306<sub>9</sub>, 2.221<sub>9</sub>, 4.227;  
 2.309<sub>5</sub>, 2.182<sub>0</sub>, 4.249; 2.312<sub>2</sub>, 2.146<sub>1</sub>, 4.273; 2.314<sub>8</sub>, 2.113<sub>9</sub>, 4.297; 2.317<sub>3</sub>, 2.084<sub>4</sub>, 4.324;  
 2.319<sub>8</sub>, 2.057<sub>5</sub>, 4.353; 2.322<sub>2</sub>, 2.033<sub>0</sub>, 4.385; 2.324<sub>6</sub>, 2.010<sub>5</sub>, 4.420; 2.326<sub>9</sub>, 1.989<sub>8</sub>, 4.461;  
 2.329<sub>0</sub>, 1.971<sub>1</sub>, 4.504; 2.331<sub>2</sub>, 1.953<sub>8</sub>, 4.557; 2.333<sub>1</sub>, 1.938<sub>6</sub>, 4.617; 2.334<sub>9</sub>, 1.925<sub>2</sub>, 4.710;  
 2.336<sub>5</sub>, 1.913<sub>9</sub>, 4.833

$B_0 = 0.00977$  M: ( $-\log B$ ,  $-\log A$ ,  $p[H]$ ) curve 3 of Figure 1;  
 -2.010<sub>1</sub>,  $A = 0$ , 3.479; 2.010<sub>3</sub>, 4.426<sub>1</sub>, 3.490; 2.010<sub>6</sub>, 3.939<sub>8</sub>, 3.528; 2.011<sub>2</sub>, 3.573<sub>8</sub>, 3.586;  
 2.012<sub>1</sub>, 3.344<sub>0</sub>, 3.639; 2.013<sub>4</sub>, 3.114<sub>0</sub>, 3.719; 2.014<sub>9</sub>, 2.955<sub>6</sub>, 3.775; 2.016<sub>7</sub>, 2.818<sub>4</sub>, 3.826;  
 2.018<sub>7</sub>, 2.703<sub>9</sub>, 3.870; 2.021<sub>0</sub>, 2.606<sub>0</sub>, 3.910; 2.023<sub>3</sub>, 2.522<sub>9</sub>, 3.942; 2.025<sub>8</sub>, 2.449<sub>5</sub>, 3.969;  
 2.028<sub>4</sub>, 2.384<sub>5</sub>, 3.991; 2.031<sub>1</sub>, 2.326<sub>7</sub>, 4.011; 2.033<sub>8</sub>, 2.275<sub>3</sub>, 4.019; 2.036<sub>7</sub>, 2.226<sub>0</sub>, 4.039;  
 2.039<sub>4</sub>, 2.185<sub>1</sub>, 4.056; 2.042<sub>1</sub>, 2.147<sub>8</sub>, 4.061; 2.045<sub>0</sub>, 2.112<sub>3</sub>, 4.073; 2.047<sub>8</sub>, 2.080<sub>0</sub>, 4.085;  
 2.050<sub>6</sub>, 2.050<sub>6</sub>, 4.099; 2.053<sub>3</sub>, 2.023<sub>9</sub>, 4.111; 2.056<sub>0</sub>, 1.998<sub>5</sub>, 4.124; 2.058<sub>7</sub>, 1.975<sub>0</sub>, 4.137;  
 2.061<sub>4</sub>, 1.952<sub>9</sub>, 4.151; 2.064<sub>1</sub>, 1.932<sub>4</sub>, 4.165; 2.066<sub>7</sub>, 1.913<sub>0</sub>, 4.179; 2.069<sub>3</sub>, 1.894<sub>7</sub>, 4.195;  
 2.071<sub>9</sub>, 1.877<sub>4</sub>, 4.210; 2.074<sub>4</sub>, 1.861<sub>0</sub>, 4.227; 2.076<sub>9</sub>, 1.845<sub>5</sub>, 4.243; 2.079<sub>5</sub>, 1.830<sub>7</sub>, 4.262;  
 2.081<sub>9</sub>, 1.816<sub>8</sub>, 4.281; 2.084<sub>4</sub>, 1.803<sub>5</sub>, 4.301; 2.086<sub>8</sub>, 1.790<sub>8</sub>, 4.324; 2.089<sub>1</sub>, 1.778<sub>8</sub>, 4.345;  
 2.091<sub>5</sub>, 1.767<sub>2</sub>, 4.370; 2.093<sub>7</sub>, 1.756<sub>3</sub>, 4.399; 2.096<sub>0</sub>, 1.746<sub>0</sub>, 4.427; 2.098<sub>2</sub>, 1.736<sub>1</sub>, 4.460;  
 2.100<sub>3</sub>, 1.726<sub>8</sub>, 4.498; 2.102<sub>3</sub>, 1.718<sub>2</sub>, 4.537; 2.104<sub>3</sub>, 1.709<sub>8</sub>, 4.588; 2.106<sub>1</sub>, 1.702<sub>6</sub>, 4.641;  
 2.107<sub>0</sub>, 1.698<sub>9</sub>, 4.660

$B_0 = 0.02070$  M: ( $-\log B$ ,  $-\log A$ ,  $p[H]$ ) curve 4 of Figure 1;  
 1.684<sub>0</sub>,  $A = 0$ , 3.294; 1.684<sub>6</sub>, 3.842<sub>3</sub>, 3.331; 1.685<sub>6</sub>, 3.426<sub>4</sub>, 3.390; 1.686<sub>9</sub>, 3.170<sub>5</sub>, 3.449;  
 1.689<sub>0</sub>, 2.997<sub>6</sub>, 3.514; 1.691<sub>6</sub>, 2.762<sub>1</sub>, 3.583; 1.694<sub>3</sub>, 2.630<sub>7</sub>, 3.634; 1.697<sub>2</sub>, 2.516<sub>0</sub>, 3.677;  
 1.700<sub>9</sub>, 2.417<sub>5</sub>, 3.719; 1.704<sub>5</sub>, 2.335<sub>3</sub>, 3.756; 1.708<sub>3</sub>, 2.261<sub>9</sub>, 3.787; 1.712<sub>2</sub>, 2.201<sub>4</sub>, 3.815;  
 1.716<sub>2</sub>, 2.145<sub>9</sub>, 3.840; 1.720<sub>2</sub>, 2.096<sub>3</sub>, 3.861; 1.724<sub>4</sub>, 2.051<sub>6</sub>, 3.880; 1.728<sub>6</sub>, 2.011<sub>1</sub>, 3.898;  
 1.732<sub>7</sub>, 1.974<sub>1</sub>, 3.914; 1.736<sub>9</sub>, 1.940<sub>4</sub>, 3.929; 1.741<sub>1</sub>, 1.909<sub>4</sub>, 3.943; 1.745<sub>3</sub>, 1.880<sub>8</sub>, 3.956;  
 1.753<sub>9</sub>, 1.827<sub>8</sub>, 3.967; 1.758<sub>0</sub>, 1.804<sub>6</sub>, 3.978; 1.766<sub>3</sub>, 1.763<sub>1</sub>, 4.001; 1.774<sub>2</sub>, 1.726<sub>8</sub>, 4.024;  
 1.782<sub>1</sub>, 1.694<sub>3</sub>, 4.057; 1.789<sub>8</sub>, 1.665<sub>2</sub>, 4.071; 1.797<sub>3</sub>, 1.638<sub>9</sub>, 4.095; 1.804<sub>7</sub>, 1.615<sub>1</sub>, 4.121;  
 1.811<sub>9</sub>, 1.593<sub>2</sub>, 4.149; 1.819<sub>0</sub>, 1.573<sub>2</sub>, 4.177; 1.826<sub>0</sub>, 1.554<sub>7</sub>, 4.208; 1.832<sub>7</sub>, 1.537<sub>8</sub>, 4.230;  
 1.839<sub>7</sub>, 1.521<sub>1</sub>, 4.264; 1.845<sub>9</sub>, 1.506<sub>9</sub>, 4.314; 1.852<sub>0</sub>, 1.493<sub>9</sub>, 4.368; 1.857<sub>7</sub>, 1.481<sub>9</sub>, 4.432;  
 1.860<sub>5</sub>, 1.476<sub>3</sub>, 4.473; 1.863<sub>1</sub>, 1.471<sub>2</sub>, 4.513; 1.865<sub>7</sub>, 1.466<sub>2</sub>, 4.569; 1.867<sub>8</sub>, 1.462<sub>0</sub>, 4.601

$B_0 = 0.04024$  M: ( $-\log B$ ,  $-\log A$ ,  $p[H]$ ) curve 5 of Figure 1;  
 1.395<sub>3</sub>,  $A = 0$ , 3.100; 1.400<sub>4</sub>, 2.928<sub>9</sub>, 3.261; 1.399<sub>4</sub>, 3.034<sub>6</sub>, 3.235; 1.402<sub>6</sub>, 2.777<sub>9</sub>, 3.308;  
 1.405<sub>6</sub>, 2.632<sub>2</sub>, 3.353; 1.409<sub>0</sub>, 2.509<sub>6</sub>, 3.398; 1.412<sub>5</sub>, 2.411<sub>2</sub>, 3.438; 1.416<sub>2</sub>, 2.328<sub>8</sub>, 3.473;  
 1.420<sub>0</sub>, 2.258<sub>2</sub>, 3.505; 1.423<sub>8</sub>, 2.196<sub>3</sub>, 3.532; 1.431<sub>9</sub>, 2.092<sub>8</sub>, 3.582; 1.440<sub>0</sub>, 2.009<sub>7</sub>, 3.624;  
 1.452<sub>3</sub>, 1.910<sub>0</sub>, 3.677; 1.464<sub>6</sub>, 1.831<sub>1</sub>, 3.720; 1.476<sub>8</sub>, 1.766<sub>8</sub>, 3.756; 1.489<sub>0</sub>, 1.712<sub>2</sub>, 3.783;  
 1.500<sub>8</sub>, 1.666<sub>5</sub>, 3.803; 1.512<sub>5</sub>, 1.626<sub>2</sub>, 3.825; 1.523<sub>9</sub>, 1.591<sub>3</sub>, 3.846; 1.535<sub>0</sub>, 1.560<sub>7</sub>, 3.868;  
 1.545<sub>9</sub>, 1.533<sub>2</sub>, 3.877; 1.556<sub>5</sub>, 1.508<sub>7</sub>, 3.900; 1.570<sub>1</sub>, 1.480<sub>0</sub>, 3.928; 1.589<sub>3</sub>, 1.454<sub>3</sub>, 3.957;  
 1.596<sub>1</sub>, 1.431<sub>5</sub>, 3.986; 1.608<sub>6</sub>, 1.411<sub>1</sub>, 4.016; 1.620<sub>7</sub>, 1.392<sub>8</sub>, 4.047; 1.632<sub>3</sub>, 1.376<sub>1</sub>, 4.081;  
 1.643<sub>7</sub>, 1.361<sub>0</sub>, 4.117; 1.654<sub>8</sub>, 1.346<sub>9</sub>, 4.140; 1.665<sub>4</sub>, 1.334<sub>3</sub>, 4.195; 1.670<sub>5</sub>, 1.328<sub>5</sub>, 4.224;  
 1.675<sub>5</sub>, 1.322<sub>9</sub>, 4.255; 1.680<sub>5</sub>, 1.317<sub>5</sub>, 4.290; 1.685<sub>2</sub>, 1.312<sub>4</sub>, 4.331; 1.690<sub>0</sub>, 1.307<sub>6</sub>, 4.376;  
 1.694<sub>0</sub>, 1.303<sub>1</sub>, 4.431; 1.696<sub>4</sub>, 1.300<sub>9</sub>, 4.463

---

the measured cell was



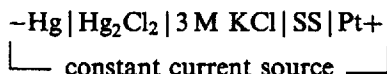
in which RE represents the two Ag/AgCl(s) internal reference electrodes of the combined glass electrode. It is assumed that the liquid junction potential arising at the interface 3 M KCl | TS is negligible owing to the very slight difference in composition of the contacting solutions. Under the present experimental conditions the p[H] of the test solution can be expressed simply by (1).

$$p[\text{H}] = p[\text{H}]_{\text{as}} - \frac{E_G}{U_N} \quad (1)$$

In (1)  $E_G$  represents the potential of cell (G) and  $U_N$  is the Nernst potential at 30°C. The constant  $p[\text{H}]_{\text{as}}$  was determined frequently during a titration by measuring the potential of the combined glass electrode in a standard solution, SS, of composition

$$\text{SS} = 0.00100 \text{ M HCl}, \quad 3.000 \text{ M KCl}.$$

This standard solution, to which  $p[\text{H}]_{\text{SS}} = 3.000 \pm 0.004$  is attributed, was prepared by generating an accurately known amount of  $\text{H}^+$  in a 3.000 M KCl solution by a constant current coulometric technique using the circuit below.



In order to assess the correct functioning of the glass electrode, a conventional acid–base titration of a solution of HCl in 3.000 M KCl with the titrating solution T was performed from time to time. Evaluation of the data *via* a Gran diagram<sup>10,11</sup> always confirmed that the combined glass electrode conformed very closely to the Nernstian slope. By very careful manipulation of the glass electrode we succeeded in keeping  $p[\text{H}]_{\text{as}}$  variations within 0.01 units ( $\cong 0.6 \text{ mV}$ ) throughout the whole measurement time. The accuracy of our p[H] measurements,  $\Delta p[\text{H}]$ , should be not less than  $\pm 0.004$  units, namely the accuracy of the p[H] of the standard solution SS.

### Materials and Analysis

The starting aluminum solution  $\text{TS}_0$  was prepared from an  $\text{AlCl}_3$  stock solution obtained by dissolving metallic Al wire (Fluka 99.999%) in

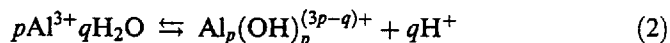


conc. HCl (Fluka p.a.) and analysed by standard methods. The titrant solution, T, was prepared by diluting a carbonate-free saturated solution of KOH with boiled bi-distilled water under an N<sub>2</sub> stream and adding a suitable amount of solid KCl. The KOH solution was analysed by conventional methods and was stored away from contact with air in a polyethylene bottle. KCl, employed to make up the ionic medium, was Fluka ACS (>99.8%) and was tested for metallic trace impurities before use. A 3 M KCl solution, tested according to the method presented in Ref. 10, was found to contain less than 10<sup>-5</sup> M protolytic impurities.

## RESULTS AND DISCUSSION

The analysis of the integral titration curves of Figure 1 is straightforward. The reason is simply that we have practically measured the whole acid–base titration curves of Al<sup>3+</sup>. This is seldom the case since conventionally only short segments of the titration curves, referring to slightly hydrolysed solutions (small *f*) are available and this makes uncertain the detection of species with a high OH<sup>-</sup> to metal ratio.

Even a superficial inspection of the integral titration curves of Figure 1 shows that Al<sup>3+</sup> solutions have a high buffer capacity at *f* values between ≈0.5 and ≈2.2, and this leaves no doubt that a reaction takes place rapidly between Al<sup>3+</sup> and the added base. On the other side the titration curves converge, by increasing p[H], towards a single *f* value which apparently is somewhat higher than 2.65. This is a convincing evidence that a single species, having OH<sup>-</sup> to metal ratio not far from 2.65, is ultimately formed. Obviously, this species is not Al<sub>13</sub>(OH)<sub>32</sub><sup>7+</sup> which has a theoretical ligand to metal ratio of only 2.46. This of course does not imply that the “12,32” cation is not formed at lower *f* values. Apart from these qualitative and very evident aspects of the titration curves, the problem is to find the minimum number of reactions:



which need to be postulated and their equilibrium constants

$$\beta_{pq} = \frac{[\text{Al}_p(\text{OH})_q^{(3p-q)+}][\text{H}^+]^q}{[\text{Al}^{3+}]^p} \quad (3)$$

in order to reproduce the observed titration curves within the accuracy of the present measurements. The following strategy has been employed.

We started by analysing the curve at  $B_0 = 0.00548$  M (curve 2 in Figure 1), which exposes the highest  $f$  value measured, by means of the titration curves simulation program HYSS which is part of the HYPERQUAD 2000 software program suite.<sup>12</sup> In this way a limited number of plausible models, each made up of a few species and the corresponding  $\beta_{pq}$  constants were generated. All these models gave a more or less acceptable fit of the titration data at  $B_0 = 0.00548$  M. The degree to which an assumed model and set of equilibrium constants reproduced the experimental profile could be judged either by visually comparing the theoretical and experimental curves, or from the  $\sigma^2$  value, *i.e.*, the scaled and weighted differences of the squares of measured and calculated  $p[H]$ , (4).

$$\sigma^2 = \frac{1}{N} \sum_i W_i \left( p[H]_{\text{calc}} - p[H]_{\text{exp}} \right)^2 \quad (4)$$

In (4)  $N$  is the number of points describing the experimental curve and  $W_i$  is the weight attributed to point  $i$ . Since we used a weighting scheme with

$$W_i = \frac{1}{(\Delta p[H])^2} \quad (5)$$

where  $\Delta p[H]$  is the presumed accuracy of our  $p[H]$  measurements, it follows that an acceptable model is one that gives  $\sigma^2 \cong 1$ . We tested practically every combination of the described species. Each of the restricted number of models was then used in turn to fit the remaining titration curves, except the titration at  $B_0 = 0.04024$  M (curve 5 in Figure 1), which was not considered for the reasons mentioned above.

For each curve the  $\beta_{pq}$  constants belonging to a given model were varied to obtain  $\sigma^2 \cong 1$ . As a result of this procedure a model gives four sets of  $\beta_{pq}$  values, one for each titration curve. Thus,  $\bar{\beta}_{pq}$ , the average value of the four equilibrium constants referring to species  $(p, q)$  in a given model, and the maximum deviation from average,  $\Delta_{pq}^{\text{max}}$ , defined as the largest  $\beta_{pq} - \bar{\beta}_{pq}$  difference over the four  $\beta_{pq}$  values were then calculated. At the end, to each of the selected models an array of  $\bar{\beta}_{pq} \pm \Delta_{pq}^{\text{max}}$  values was attributed. Finally we selected the model containing the species  $Al_2(OH)_2^{4+}$ ,  $Al_3(OH)_6^{3+}$ ,  $Al_{13}(OH)_{32}^{7+}$  and  $Al_{13}(OH)_{35}^{4+}$ , which by far gives  $\bar{\beta}_{pq}$  values with the lowest  $\Delta_{pq}^{\text{max}}$  value. The four sets of formation constants obtained for each of the titration curves of Figure 1 and the corresponding  $\sigma^2$  values are reported in the first four rows of Table II; the last row reports the average  $\bar{\beta}_{pq}$  and the corresponding  $\Delta_{pq}^{\text{max}}$  which we assume as the uncertainty on the

corresponding constant. The full curves in Figure 1 have been evaluated by using the average values reported in Table II.

As expected, from the observed drift of the  $p[H]$  towards acidic values, the curve referring to the titration at  $B_0 = 0.04024 M$  lies somewhat under the corresponding theoretical curve. Nevertheless it shows the same shape and apparently approaches the same asymptote at  $f = 2.69$ , corresponding to the  $OH^-$  to  $Al^{3+}$  ratio of the species  $Al_{13}(OH)_{35}^{4+}$ .

A distribution diagram of the four species detected in this work as a function of  $p[H]$ , for a 20 mM Al(III) solution, is presented in Figure 2. Although the "13, 32" cation still dominates  $Al^{3+}$  hydrolysis in agreement with current views, we, unfortunately, had to add two undescribed species, *i.e.*,  $Al_3(OH)_6^{3+}$  and  $Al_{13}(OH)_{35}^{4+}$ , to the already long list of aluminum hydroxo complexes.

TABLE II Survey of the equilibrium constants calculations. The fifth row reports the final values of the equilibrium constants of reaction (2); the uncertainties are maximum deviations

$B_0$ , mM	$\log \beta_{2,2}$	$\log \beta_{3,6}$	$\log \beta_{13,32}$	$\log \beta_{13,35}$	$\sigma^2$
2.53	-6.59	-21.23	-104.47	-117.71	1.17
5.25	-6.67	-20.96	-104.46	-117.71	1.01
9.77	-6.70	-20.78	-104.36	-117.83	0.76
20.70	-6.78	-20.62	-104.55	-117.86	1.94
Av:	$-6.68 \pm 0.09$	$-20.90 \pm 0.30$	$-104.45 \pm 0.10$	$-117.78 \pm 0.08$	

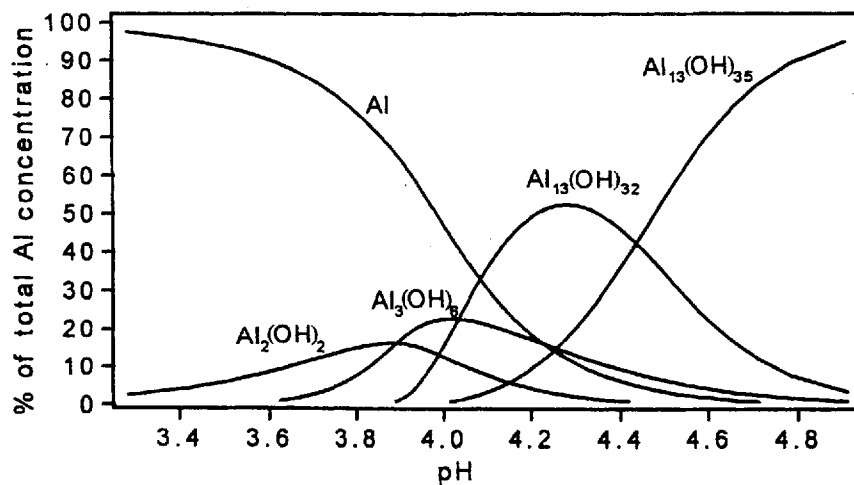


FIGURE 2 Distribution diagram of the four  $Al_p(OH)_q^{(3p-q)+}$  species detected in this work. The diagram has been drawn assuming an Al(III) concentration of 20 mM and the equilibrium constants of Table II. Charges are omitted.

In particular,  $\text{Al}_{13}(\text{OH})_{35}^{4+}$ , which obviously is produced from the dissociation of the parent polyacid  $\text{Al}_{13}(\text{OH})_{32}^{7+}$ , must be postulated to account for the common asymptote of our titration curves at high  $\text{p}[\text{H}]$ , and  $\text{Al}_3(\text{OH})_6^{3+}$  takes the place of  $\text{Al}_3(\text{OH})_4^{5+}$ , which is most frequently described.<sup>1,7</sup> Although this will not deeply affect the common manipulations of  $\text{Al}^{3+}$  hydrolysed solutions, it may change somewhat our view on the mechanism of formation of the "13, 32" cation. In fact in the mechanism suggested by Wood and coworkers,<sup>5</sup> the complex  $[\text{Al}_3(\text{tris-}\mu\text{-OH})(\text{OH})_3]^{5+}$ , to which the very compact structure of Figure 3A is attributed, plays a central role.

According to these authors<sup>5</sup>  $[\text{Al}_3(\text{tris-}\mu\text{-OH})(\text{OH})_3]^{5+}$  is the monomer which initiates the condensation process which ultimately produces  $\text{Al}_{13}(\text{OH})_{32}^{7+}$ .  $[\text{Al}_3(\text{tris-}\mu\text{-OH})(\text{OH})_3]^{5+}$  first dissociates to  $[\text{Al}_3(\text{tris-}\mu\text{-O})(\text{OH})_3]^{4+}$ , then one of the aluminum cations assumes tetrahedral coordination, as found for the central  $\text{Al}^{3+}$  ion in the bulk structure of  $\text{Al}_{13}(\text{OH})_{32}^{7+}$  (Figure 3B). Supposedly, this change of coordination geometry takes place slowly, but once accomplished, condensation of monomeric and additional trimeric hydroxo species, around the trimer with the tetrahedrally coordinated Al, rapidly creates the "13, 32" cation. In contrast with this, Akitt and Farthing,<sup>13</sup> conducted an  $^{27}\text{Al}$  NMR investigation of hydrolysed  $\text{Al}^{3+}$  solutions prepared by rapidly mixing an acidic  $\text{AlCl}_3$  solution with concentrated ( $> 1 \text{ M}$ )  $\text{Na}_2\text{CO}_3$ , much in the same way as we did during our integral titrations, suggested an alternative mechanism to explain their observations. They maintain that, under their conditions, a tetrahedrally coordinated  $\text{Al}(\text{OH})_4^-$  species is immediately formed upon mixing the solutions because of a local excess of base. Rapid condensation of six  $\text{Al}_2(\text{OH})_2^{4+}$  around the transient  $\text{Al}(\text{OH})_4^-$  produces  $\text{Al}_{13}(\text{OH})_{32}^{7+}$ .

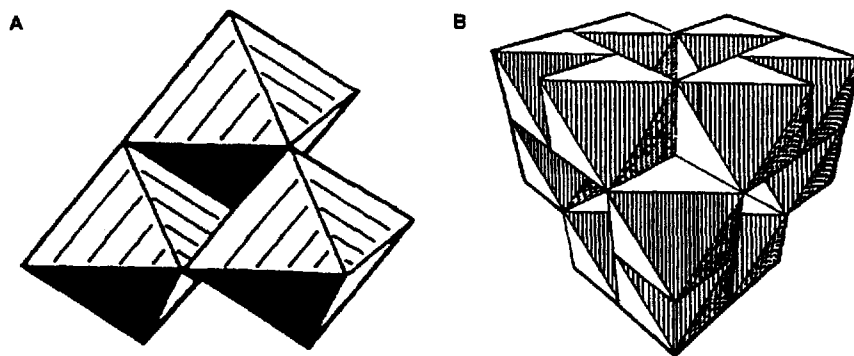
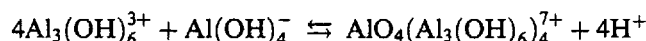


FIGURE 3 A: The compact structure of the  $[\text{Al}_3(\text{tris-}\mu\text{-OH})(\text{OH})_3]^{5+}$  according to Wood,<sup>5</sup> B: The bulky structure of  $\text{Al}_{13}(\text{OH})_{32}^{7+}$  from X-ray crystallography.<sup>9</sup>

It seems to us that the views of Akitt and Farthing, although strongly criticized, are supported by the results of this paper. Indeed, the rarely employed integral titration procedure adopted by us makes a local excess of  $\text{OH}^-$ , on mixing the slightly acidic  $\text{Al}^{3+}$  solution with 0.1 M KOH, very likely and the production of appreciable, although transient,  $\text{Al}(\text{OH})_4^-$  not unreasonable.

According to us, the "13, 32" cation could be created simply by condensation of four  $\text{Al}_3(\text{OH})_6^{3+}$  around  $\text{Al}(\text{OH})_4^-$  in the manner shown below



During this reaction the  $\text{Al}(\text{OH})_4^-$  ion is forced to assume tetrahedral coordination because of the very bulky structure of  $\text{AlO}_4(\text{Al}_3(\text{OH})_6)_4^{7+}$  cation. This mechanism may also explain the divergent observations on the speed of formation of the "13, 32" cation which is reported<sup>1</sup> to depend both on the concentration of the titrating base and the way it is added. The rapid formation of  $\text{AlO}_4(\text{Al}_3(\text{OH})_6)_4^{7+}$  during our integral titrations, as testified by the high buffering capacity of  $\text{Al}^{3+}$  solutions, seems to show that rapid addition of a concentrated base is a condition for rapid equilibrium in the solution.

In continuing work an  $^{27}\text{Al}$  NMR investigation of hydrolysed aluminum solutions will be undertaken to further test these views.

### References

- [1] C.F. Baes, Jr. and R.E. Mesmer, *The Hydrolysis of Cations* (Krieger Publishing Company, Malabar, Florida, 1976).
- [2] E. Marklund and L.-O. Öhman, *Acta Chem. Scand.*, **44**, 228 (1990).
- [3] T. Hedlund, S. Sjöberg and L.-O. Öhman, *Acta Chem. Scand.*, **A41**, 197 (1987).
- [4] P. Djurdjevic and R. Jelic, *Main Group Metal Chem.*, **21**, 331 (1998).
- [5] C.J. Brinker and G.B. Scherer, *Sol-Gel Science* (Academic Press Inc., San Diego, CA, 1990).
- [6] Hyuk Choi, Young-UK Kwon and Oc Hee Han, *Chem. Mater.*, **11**, 1641 (1999).
- [7] Stability Constant Database, SCQuery Version 1.37 (IUPAC and Academic Software, 1993).
- [8] R.E. Mesmer and C.F. Baes, Jr., *Inorg. Chem.*, **10**, 2290 (1971).
- [9] G. Johansson, *Ark. Kemi*, **27**, 321 (1963).
- [10] A.E. Martell and R.J. Motekaitis, *Determination and Use of Stability Constants* (VCH Publishers, Inc., New York, 1990).
- [11] G. Gran, *Analyst*, **77**, 661 (1952).
- [12] P. Gans, A. Sabatini and A. Vacca, *Talanta*, **43**, 1739 (1996).
- [13] J.W. Akitt and A. Farthing, *J. Chem. Soc., Dalton*, 1617 (1981).